Chapter VII

CHAPTER VII

EFFECT OF ROTATION ON THE LINEAR STABILITY OF PARALLEL STRATIFIED SHEAR FLOWS

7.1 Introduction

Shear flows subjected to system rotation, where the rotation axis is parallel have many interesting features. The Coriolis force has a strong effect on the flow field even at low rotational speeds. Various natural phenomena and technological situations are directly governed by the action of Coriolis force.

The rotational instability of an inviscid homogeneous fluid was first studied by Rayleigh (1917). He developed the general linear stability theory for inviscid parallel flows and showed that a necessary condition for instability is the velocity profile with no point of inflection. Synge (1933) examined the stability of a steady rotation of heterogeneous fluids with the action of body force. The rotational instability of a stratified rotating fluid by means of linearised perturbation equations assuming the basic horizontal flow was studied by Ken Sasaki (1971). He also assumed that horizontal layer is confined in a thin layer.

Mobbs and Darby (1989) obtained a general method to test the stability of a stratified, parallel shear flow. The observation of shear flow instability in a rotating system with a soap membrane was analyzed by Couder (1981). The primary instability of an azimuthal jet in a rotating annulus with rigid upper lid and a sloping bottom was studied experimentally by Solomon *et al* (1993). An asymptotic approach to examine the linear stability of plane parallel shear flow in a rotating system with respect to long wave disturbances was developed by Sumathi and Ragavachar (1993). Paul Matthews and Stephen Cox (1997) analyzed the convective stability in a rotating shear flow.

The linear stability of a rotating stratified inviscid horizontal plane Couette flow in a channel was studied in the limit of strong rotation and stratification by Vanneste and Yavneh (2007). Kloosterziel *et al* (2007) obtained the saturation of inertial instability in rotating planar shear flows. Arobone and Sarkar (2012) investigated the instability mechanisms for a horizontal shear layer with uniform stable stratification rotating about a vertical axis. The linear instability of rotating, stably stratified, vertical shear flows $U(z)$ with Boussinesq approximation was

studied by Wang et. al (2014). Three-dimensional rotating Couette flow using the generalized quasilinear approximation was analyzed by Tobias and Marston (2017). Facchini et. al (2018) presented the stability analysis of plane Couette flow which is stably stratified in the vertical direction, orthogonal to the horizontal shear.

Motivated by the astrophysical applications, in this chapter, the work of Sumathi and Ragavachar (1993) is extended to stratified shear layer by assuming the basic velocity profile as linear. The mathematical treatment includes the linearized equations of motion for infinitesimal disturbances to an unsteady stratified parallel shear flow of an inviscid, incompressible rotating flow. The effect of rotation on the linear stability of parallel stratified shear flow between two rigid plates at $z = \pm L$ is analyzed for asymptotically small wave numbers.

7.2 Mathematical formulation

Consider the three dimensional shear flow of an inviscid, incompressible Boussinesq fluid with constant Brunt-Vaisala frequency N^2. Assume that the domain rotates around z-axis, it is unbounded in the x and y-directions, and bounded in the z-direction by two rigid walls separated by a distance $2L$. The fluid is assumed to be nondiffusive and inviscid.

The assumptions made for the present problem are:

- Flow of unsteady, inviscid, stratified, Newtonian fluid is considered.
- Fluid is flowing between two horizontal infinite rigid plates at a distance $2L$ apart.
- The fluid is assumed to be rotating about a vertical axis with angular velocity Ω.
- No slip boundary conditions are imposed at the boundaries.
- Boussinesq approximation is applied in the momentum equation.
- All the fluid properties are assumed constant except the density variation which takes place with vertical coordinate z due to stratification.
- The basic velocity profile is assumed as $\vec{q}_e = (U(z), 0, 0)$
- Magnetic effect and viscous dissipation effects are neglected.

Based on the assumption taken the geometrical representation of the problem is given in Figure. 7.1.

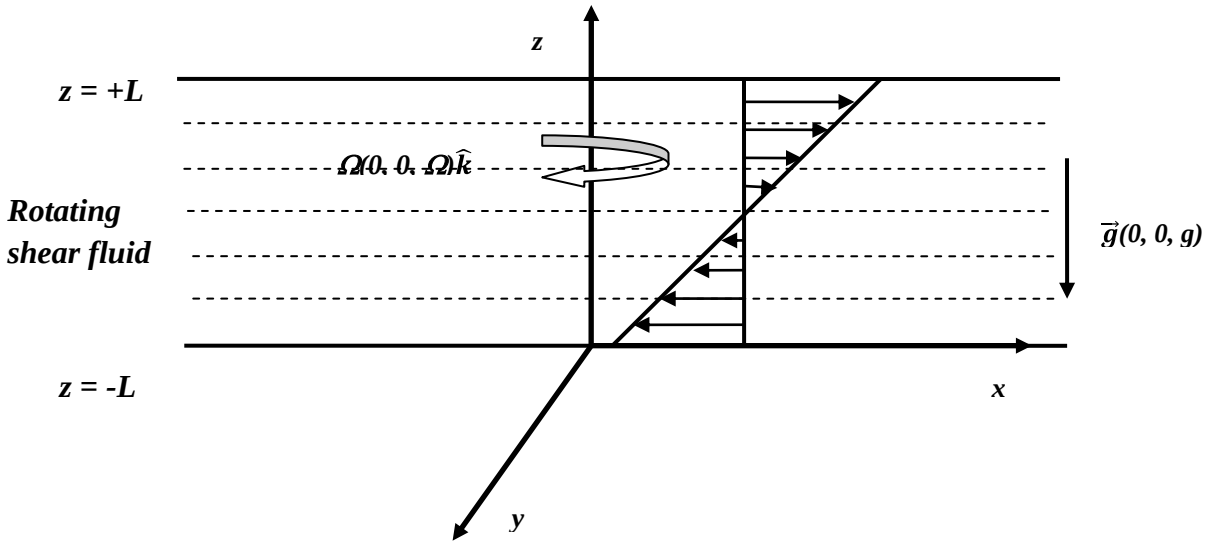

Figure 7.1. Schematic diagram of stratified shear flow with velocity (U(z), 0, 0)

Hence, the governing equations for the motion of an inviscid, incompressible rotating Boussinesq stratified fluid confined between two horizontal infinite rigid planes situated at $z = \pm L$ are

$$\nabla.\vec{q} = 0 \tag{7.1}$$

$$\rho\left(\frac{\partial\vec{q}}{\partial t} + (\vec{q}.\nabla)\vec{q} + 2\Omega\hat{k}\times\vec{q}\right) = -\nabla p - \rho g\hat{k} \tag{7.2}$$

$$\frac{\partial\rho}{\partial t} + (\vec{q}.\nabla)\rho = 0 \tag{7.3}$$

where $\vec{q}(u,v,w)$ is the velocity vector, ρ is the density of the fluid, p is the pressure and g is the acceleration due to gravity respectively.

The boundary conditions are

$$\vec{q}\,(z) = 0 \quad \text{at } z = \pm L \tag{7.4}$$

The basic flow is given by $\overrightarrow{q_e} = (U(z), 0, 0)$. At the equilibrium state, the density and pressure are related by

$$2\Omega\rho_0\hat{k}\times\overrightarrow{q_e} = -\frac{\partial p_0}{\partial z} - g\rho_0(z) \tag{7.5}$$

We use the following dimensionless variables

$$t = \frac{Lt^*}{U_0},\ (\vec{q} = U_0\vec{q}^*\ \ p = \rho_0 U_0^2 p^*,\ \rho = \frac{\rho_0 U_0^2 N_0^2}{Lg}\rho^*$$

and $(x,y,z) = L(x^*,y^*,z^*)$, (7.6)

where, $N^2 = -\frac{g}{\rho_0}\left(\frac{d\rho}{dz}\right)$ is the Brunt-Vaisala frequency which is assumed to be positive for static stability and N_0 is a typical value of Brunt-Vaisala frequency in the flow domain, L is the characteristic length and U_0 is the characteristic velocity.

The dimensionless form of the governing equations (7.1) – (7.3) are obtained as

$$\nabla.\vec{q} = 0 \quad (7.7)$$

$$\frac{\partial \vec{q}}{\partial t} + (\vec{q}.\nabla)\vec{q} = -\nabla p - \mathrm{Ri}\, g\hat{k} \quad (7.8)$$

$$\frac{\partial \rho}{\partial t} + \vec{q}.\nabla\rho = 0 \quad (7.9)$$

The asterisks that denote dimensional variables are dropped for their dimensionless counterparts.

The dimensionless boundary conditions become

$$\vec{q}\,(\pm 1) = 0 \quad (7.10)$$

Now perturb the basic state by considering the perturbed velocity components as *(U(z)+u', v', w')*, perturbed density as $\rho_0(z) + \rho'(z)$ and perturbed pressure as $p_0(z) + p'(z)$. Substituting these in the basic equations and linearizing, we obtain the following set of equations

$$\frac{\partial u'}{\partial x} + \frac{\partial v'}{\partial y} + \frac{\partial w'}{\partial z} = 0 \quad (7.11)$$

$$\frac{\partial u'}{\partial t} + U(z)\frac{\partial u'}{\partial x} + w'\frac{\partial U(z)}{\partial z} - \tau v' = -\frac{\partial p'}{\partial x} \quad (7.12)$$

$$\frac{\partial v'}{\partial t} + U(z)\frac{\partial v'}{\partial x} + \tau u' = -\frac{\partial p'}{\partial y} \quad (7.13)$$

$$\frac{\partial w'}{\partial t} + U(z)\frac{\partial w'}{\partial x} = -\frac{\partial p'}{\partial z} - Ri\rho' \quad (7.14)$$

$$\frac{\partial \rho'}{\partial t} + U(z)\frac{\partial \rho'}{\partial x} - \frac{\mathrm{N}^2}{\mathrm{N}_0^2}w' = 0 \quad (7.15)$$

The flow is characterized by two non-dimensional parameters: the Richardson number $Ri = \frac{g\beta L^2}{\rho_0 U_0^2}$ and Rotation number $\tau = \frac{2\Omega L}{U_0}$.

Employing normal mode approach we assume that all the variable quantities like velocity, density are proportional to $e^{ik(x+ly)+k\sigma t}$, where k and l are wave numbers in the x and y direction respectively and σ is the growth rate of the disturbance which is in general a complex constant. If k and l are real and $Re\,(\sigma) > 0$, then the small disturbance is linearly unstable. On the other hand if all such small disturbances to a plane-parallel shear flow have $Re\,(\sigma) < 0$, then the flow is linearly stable.

Based on this, the above linearized equations (7.11) – (7.15) can be modified to the following form

$$iku' + iklv' + \frac{\partial w'}{\partial z} = 0 \quad (7.16)$$

$$k(\sigma + iU)u' + w'\frac{\partial U(z)}{\partial z} - \tau v' = -ikp' \quad (7.17)$$

$$k(\sigma + iU)v' + w'\frac{\partial V(z)}{\partial z} + \tau u' = -ikIp' \quad (7.18)$$

$$k(\sigma + iU)w' = -\frac{\partial p'}{\partial z} - Ri\,\rho' \quad (7.19)$$

$$k(\sigma + iU)\rho' - \frac{N^2}{N_0^2}w' = 0 \quad (7.20)$$

Corresponding boundary conditions for the problem are

$$u'(z) = v'(z) = w'(z) = 0 \qquad at\ z = \pm 1 \quad (7.21)$$

7.3 Eigen values and eigen functions for long waves

Consider the analysis for long wave approximation (i.e) k is assumed to be small. The flow is assumed to be bounded between two plates $z = \pm L$. The basic arbitrary velocity profile for the flow is taken as linear (*U(z) = z*). We apply the series expansion in terms of wave number k in the form

$$f = f_0 + kf_1 + k^2 f_2 + \cdots \quad (7.22)$$

where f represents either one of the disturbances $u', v', w', \sigma, \rho'$ or p'.

By applying equation (7.22) into equations (7.16) to (7.20) and boundary conditions (7.21) the zeroth order approximation is given by

$$\begin{aligned} iu_0 + ilv_0 + \frac{\partial w_0}{\partial z} &= 0 \\ T(z)u_0 + w_0 &= -ip_0 \\ T(z)v_0 &= -ilp_0 \\ -\frac{\partial p_0}{\partial z} - Ri\,\rho_0 &= 0 \\ T(z)\rho_0 - \frac{N^2}{N_0^2}w_0 &= 0 \end{aligned} \quad (7.23)$$

where $T(z) = \sigma_0 + iz$

with the corresponding boundary condition

$$u_0(\pm 1) = v_0(\pm 1) = w_0(\pm 1) = 0 \quad (7.24)$$

Eliminating the above equation (7.23) in terms of w_0, we get

$$T(z)^2\frac{\partial^2 w_0}{\partial z^2} + \frac{Ri\,N^2}{{N_0}^2}(1 + l^2)w_0 = 0 \quad (7.25)$$

The solution of equation (7.25) is given by

$$w_0 = A\,T(z)^{m_1} + B\,T(z)^{m_2},$$

where $m_{1,2} = \frac{1 \pm \sqrt{\lambda}}{2}$, $\lambda = 1 - 4\,Ri\frac{N^2}{N_0^2}(1 + l^2)$, *A*, *B* are arbitrary constants.

By imposing the boundary condition that the velocity should vanish at the boundaries. The value of σ_0 can be obtained by solving equation (7.25) subject to the boundary condition $w_0 = 0 \;\; at \; z = \pm 1$,

$$\sigma_0 = i \frac{1+e^{\frac{2n\pi i}{\sqrt{1-4\,Ri\frac{N^2}{N_0^2}(1+l^2)}}}}{1-e^{\frac{2n\pi i}{\sqrt{1-4\,Ri\frac{N^2}{N_0^2}(1+l^2)}}}} \tag{7.26}$$

The solution of equation (7.23) with the boundary condition (7.24) is given as

$$\begin{aligned} u_0 &= E_7 T(z)^{m_1-1} + E_8 T(z)^{m_2-1} \\ v_0 &= E_5 T(z)^{m_1-1} + E_6 T(z)^{m_2-1} \\ w_0 &= T(z)^{m_1} + B T(z)^{m_2} \\ p_0 &= E_1 T(z)^{m_1} + E_2 T(z)^{m_2} \\ \rho_0 &= E_3 T(z)^{m_1-1} + E_4 T(z)^{m_2-1} \end{aligned} \tag{7.27}$$

The first order approximation is given by

$$\begin{aligned} iu_1 + ilv_1 + \frac{\partial w_1}{\partial z} &= 0 \\ T(z)u_1 + w_1 - i\sigma_1 u_0 - \tau v_0 &= -ip_1 \\ T(z)v_1 - i\sigma_1 v_0 + \tau u_0 &= -ilp_1 \\ -\frac{\partial p_1}{\partial z} - Ri\,\rho_1 &= 0 \\ T(z)\rho_1 - i\sigma_1\rho_0 - \frac{N^2}{N_0^2}w_1 &= 0 \end{aligned} \tag{7.28}$$

with the boundary condition

$$u_1(\pm 1) = v_1(\pm 1) = w_1(\pm 1) = 0 \tag{7.29}$$

Equation (7.28) is simplified in terms of w_1 as

$$\begin{aligned} T(z)^2 \frac{\partial^2 w_1}{\partial z^2} - \frac{Ri\,N^2}{{N_0}^2}(1+l^2)w_1 = -\sigma_1 \left(T(z)\frac{\partial^2 w_0}{\partial z^2}\right) - i\tau\left(\frac{\partial v_0}{\partial z} - l\frac{\partial u_0}{\partial z}\right)T(z) \\ -Ri\rho_0\sigma_1\,(1+l^2) \end{aligned} \tag{7.30}$$

The value of σ_1 can be obtained from the above equation by applying the boundary condition that $w_1(\pm 1) = 0$

$$\sigma_1 = \frac{-\tau\,E_{21}}{E_{22}+Ri\,E_{23}} \tag{7.31}$$

The solution of equation (7.29) with the boundary condition (7.30) is given by

$$\begin{aligned} u_1 = {} & E_{48}(\sigma_0 + iz)^{m_1-1} + E_{49}(\sigma_0 + iz)^{m_2-1} \\ & +(\sigma_1(E_{50} + Ri\,E_{51}) + \tau E_{52})(\sigma_0 + iz)^{m_2-2} \\ & +(\sigma_1(E_{53} + Ri\,E_{54}) + \tau E_{55})(\sigma_0 + iz)^{m_2-2} \end{aligned}$$

$$
\begin{aligned}
v_1 = {} & E_{40}(\sigma_0 + iz)^{m_1-1} + E_{41}(\sigma_0 + iz)^{m_2-1} \\
& +(\sigma_1(E_{42} + Ri\, E_{43}) + \tau E_{44})(\sigma_0 + iz)^{m_2-2} \\
& +(\sigma_1(E_{45} + Ri\, E_{46}) + \tau E_{47})(\sigma_0 + iz)^{m_2-2}
\end{aligned}
$$

$$
\begin{aligned}
w_1 = {} & C(\sigma_0 + iz)^{m_1} + D(\sigma_0 + iz)^{m_2} \\
& +(\sigma_1(E_9 + Ri\, E_{10}) + \tau E_{11})(\sigma_0 + iz)^{m_2-1} \\
& +(\sigma_1(E_{12} + Ri\, E_{13}) + \tau E_{14})(\sigma_0 + iz)^{m_2-1}
\end{aligned}
$$

$$
\begin{aligned}
p_1 = {} & E_{24}(\sigma_0 + iz)^{m_1} + E_{28}(\sigma_0 + iz)^{m_2} \\
& +(\sigma_1(E_{25} + Ri\, E_{26}) + \tau E_{27})(\sigma_0 + iz)^{m_2-1} \\
& +(\sigma_1(E_{29} + Ri\, E_{30}) + \tau E_{31})(\sigma_0 + iz)^{m_2-1}
\end{aligned}
$$

$$
\begin{aligned}
\rho_1 = {} & E_{32}(\sigma_0 + iz)^{m_1-1} + E_{33}(\sigma_0 + iz)^{m_2-1} \\
& +(\sigma_1(E_{34} + Ri\, E_{35}) + \tau E_{36})(\sigma_0 + iz)^{m_2-2} \\
& +(\sigma_1(E_{37} + Ri\, E_{38}) + \tau E_{39})(\sigma_0 + iz)^{m_2-2}
\end{aligned} \qquad (7.32)
$$

The second order approximation is given by

$$
\begin{aligned}
& iu_2 + ilv_2 + \frac{\partial w_2}{\partial z} && = 0 \\
& T(z)u_2 + \sigma_1 u_1 + \sigma_2 u_0 + w_2 - \tau v_1 && = -ip_2 \\
& T(z)v_2 + \sigma_1 v_1 + \sigma_2 v_0 + \tau u_1 && = -ilp_2 \\
& T(z)w_0 && = -\frac{\partial p_2}{\partial z} - Ri\, \rho_2 \\
& T(z)\rho_2 + \sigma_1\rho_1 + \sigma_2\rho_0 - \frac{N^2}{N_0^2} w_2 && = 0
\end{aligned} \qquad (7.33)
$$

with the boundary conditions

$$
u_2(\pm 1) = v_2(\pm 1) = w_2(\pm 1) = 0 \qquad (7.34)
$$

Equation (7.33) is simplified in terms of w_2 as

$$
\begin{aligned}
T(z)^2 \frac{\partial^2 w_2}{\partial z^2} - \frac{Ri\, N^2}{{N_0}^2}(1 + l^2) w_2 = {} & -\sigma_1 \left(T(z) \frac{\partial^2 w_1}{\partial z^2} \right) - \sigma_2 \left(T(z) \frac{\partial^2 w_0}{\partial z^2} \right) \\
& -i\tau \left(\frac{\partial v_1}{\partial z} - l \frac{\partial u_1}{\partial z} \right) T(z) - Ri \rho_1 \sigma_1 (1 + l^2) \\
& -Ri \rho_0 \sigma_2 (1 + l^2) + T(z) w_0
\end{aligned} \qquad (7.35)
$$

The value of σ_2 can be obtained from the above equation by applying the boundary condition that $w_2(\pm 1) = 0$

$$
\sigma_2 = \frac{\begin{pmatrix} -\sigma_1\left((\sigma_1(E_{133} + Ri\, E_{134}) + \tau E_{135}) + Ri\, (\sigma_1(E_{136} + Ri\, E_{137}) + \tau E_{138})\right) \\ -\sigma_1(E_{128} + Ri\, E_{129}) + \tau E_{130} + \tau(\sigma_1(E_{139} + Ri\, E_{140}) + \tau E_{141}) - E_{142} \end{pmatrix}}{E_{131} + Ri\, E_{132}} \qquad (7.36)
$$

For the sake of brevity the constants are given in *Appendix V*.

7.4 Result and Discussion

We have considered an inviscid, incompressible, rotating stratified shear flow of variable density ρ. The fluid is in a state of plane parallel flow characterized by a horizontal shear layer confined between two horizontal infinite rigid planes $z = \pm L$. The fluid is assumed to be rotating with constant angular velocity Ω. The influence of wave number (k), rotation number (τ) and Brunt Vaisala frequency (N^2) on the stability characteristics of the flow are analyzed. The real part of the frequency of disturbances as a function of these parameters is plotted in Figures (7.2) – (7.13).

Figure (7.2) portrays the influence of rotation number (τ) on the growth rate (σ) with increasing wave number (k). It is clear from the Figure that due to the increase in rotation number, the growth rate of the disturbances decreases thereby making the system unstable. Figure (7.3) presents the real part of the growth rate (σ) as a function of wave number for various values of l. This shows that the frequency of disturbances increases with increase in wave number k thereby increasing the region of instability.

Figure (7.4) exhibits the behavior of growth rate (σ) due to the variation in n. It is concluded that, there exists infinite number of modes for the given stability problem. In Figures (7.5) and (7.6), the influence of Brunt Vaisala frequency (N^2) and Richardson number (Ri) on the growth rate (σ) with increasing wave number is presented. It can be seen that, increase in Brunt Vaisala frequency (N^2) decreases the growth rate. With the increase in wave number, the growth rate increases for smaller values of N^2. As N^2 increases, much change does not take place in the growth rate. Hence, it can be inferred that, increase in Brunt Vaisala frequency (N^2) contributes more to the flow stability.

Figure (7.7) shows the behavior of growth rate (σ) with the increase in Brunt Vaisala frequency (N^2) for various rotation number (τ). Initially, for smaller N^2 the frequency of disturbances decreases with the increasing rotation number (τ). Hence, the flow becomes unstable. Figure (7.8) depicts the real part of growth rate (σ) vs Brunt Vaisala frequency for different values of l on the flow instability. It is shown that, initially transition occurs with the increase in l and becomes stable as Brunt Vaisala frequency (N^2) increases.

In Figure (7.9), the nature of growth rate (σ) for various Richardson number is exhibited. It is observed that, Richardson number (*Ri)* affects the stability of the flow field. On careful observation, we identified that increase in Richardson number (*Ri)* contributes to the flow stability with the increase in Brunt Vaisala frequency (N^2). Figure (7.10) discusses about the real part of the growth rate (σ) for various rotation number (τ). This Figure shows that, the frequency of disturbances decreases with increasing rotation number (τ) for smaller values of *Ri* and becomes stable as Richardson number (*Ri)* increases.

Figure (7.11) presents the behavior of growth rate (σ) due to variations in transverse wave number (*l)*. Due to increase in *l* growth rate decreases for smaller Richardson number (*Ri)*. As *Ri* increases, the growth rate becomes stable. Figure (7.12) portrays the behavior of the real part of growth rate (σ) for various wave number (*k)* with increasing Richardson number (*Ri)*. It can be seen that, increase in wave number decreases the growth rate for the case of smaller Richardson number (*Ri).* It is inferred that, as *Ri* increases, the flow becomes unstable and contributes more to the instability.

Figure (7.13) discusses about the nature of growth rate (σ) for increasing Brunt Vaisala frequency (N^2). Due to the increase in N^2, the frequency of disturbances increases till *Ri* = 0.02. Increase in *Ri* stabilizes the flow pattern whatever N^2 may be. Figures (7.14) and (7.15) present the nature of the velocity due to the variations in rotation number (τ) and wave number (*k)*. It is observed that, increase in these two parameters increases the velocity profile.

7.5 Conclusion

In this chapter, the linear stability analysis of an inviscid, incompressible parallel stratified shear fluid is analyzed. The fluid is assumed to be rotating about a vertical axis with constant angular velocity Ω. Rotation effect on a stratified shear layer is analyzed using series expansion method by assuming $k \ll 1$. Analytical expressions were found to calculate the growth rate (σ) for long waves. These expressions are evaluated numerically for linear base flow (i.e) $U(z) = z$. Significant conclusions drawn from the study are as follows.

- Due to increase in rotation number (τ) and transverse wave number (*k*) growth rate decreases thereby making the flow stable.

- Increase in Brunt vaisala frequency (N^2) and Richardson number (Ri) decreases the growth rate thereby stabilizes the flow pattern.
- Due to increase in rotation number (τ), transverse wave number (l) and Richardson number (Ri), the growth rate of disturbance decreases, thereby contributes more to the flow stability with the increase in Brunt-Vaisala frequency (N^2).
- The rotation number (τ), wave number (k and l) and Brunt- Vaisala frequency (N^2) contributes more to the stability of the flow with increasing Richarson number (Ri).
- Velocity profile increases with the increasing rotation number (τ) and transverse wave number (k).

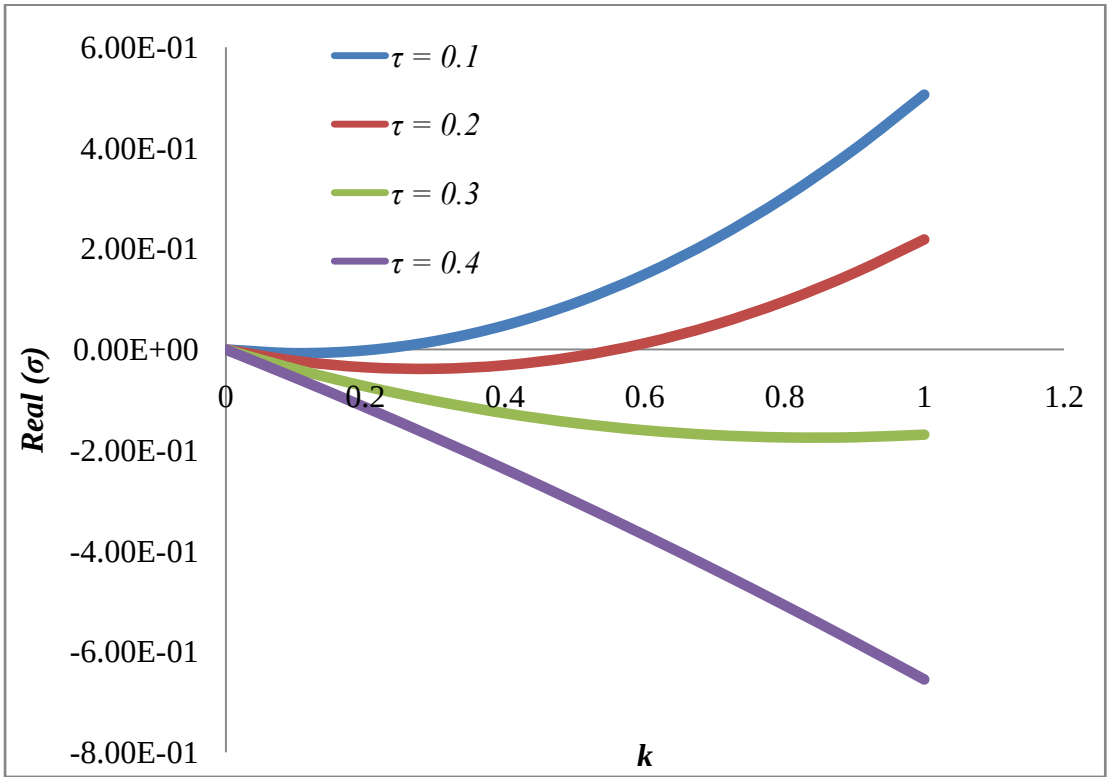

Figure 7.2 Growth rate as a function of wave number for various τ

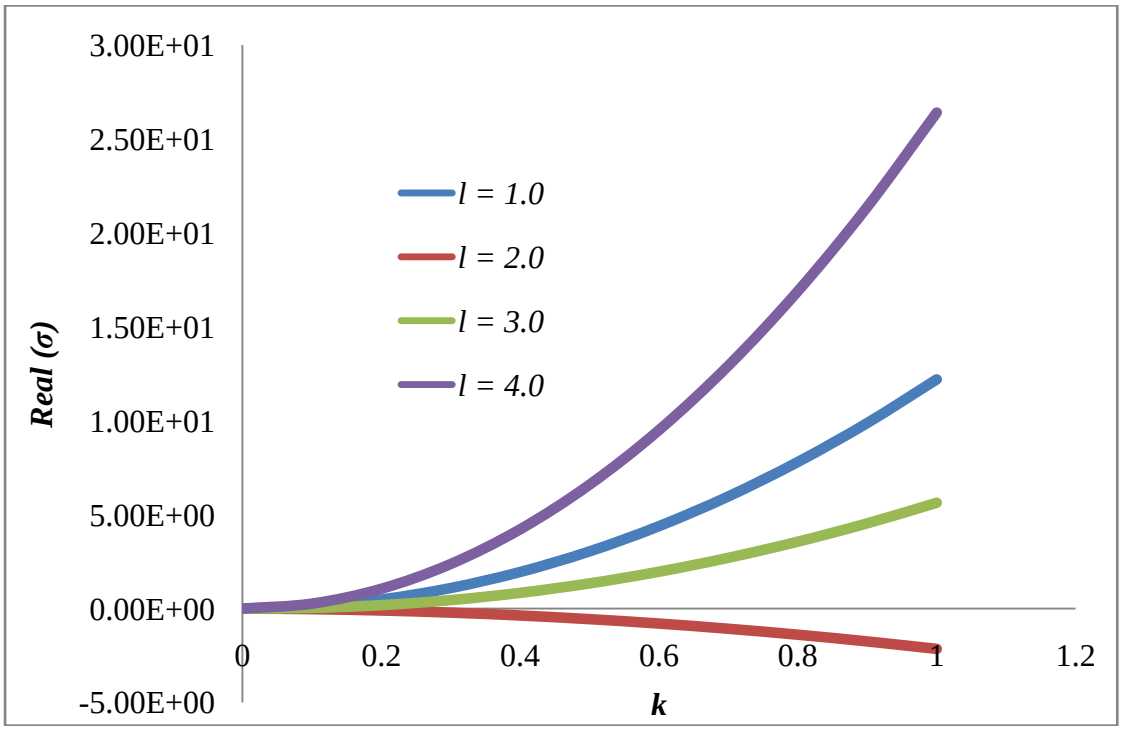

Figure 7.3 Growth rate as a function of wave number for various l

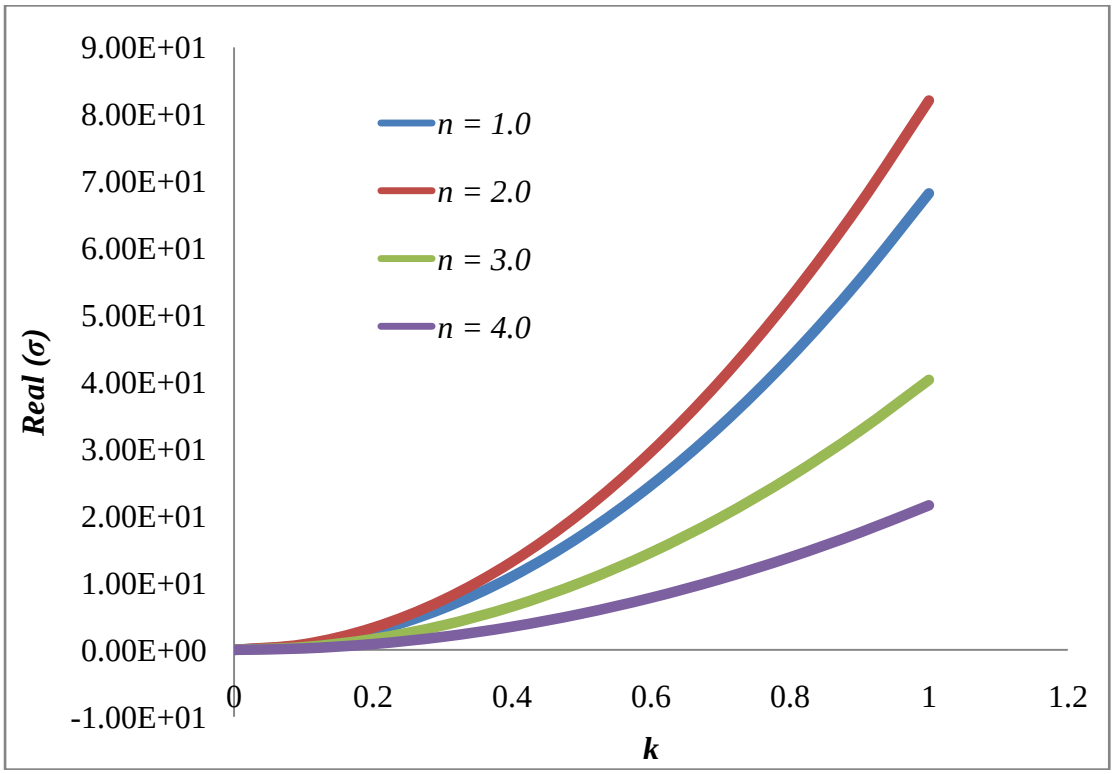

Figure 7.4 Growth rate as a function of wave number for various n

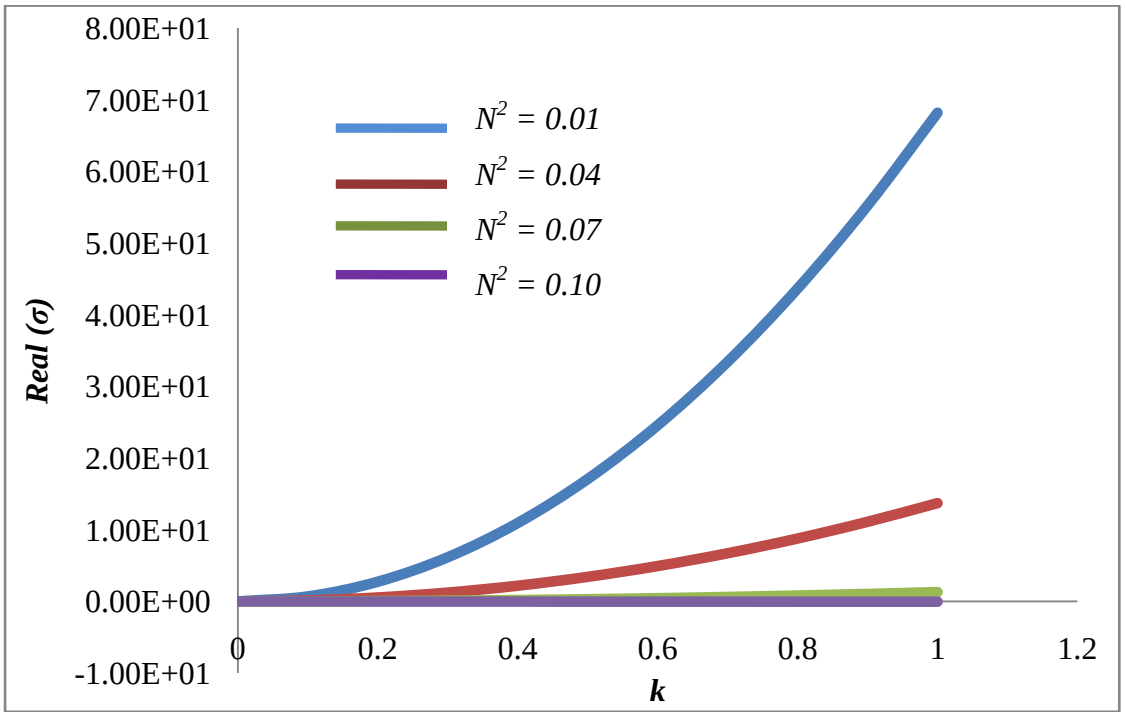

Figure 7.5 Growth rate as a function of wave number for various N^2

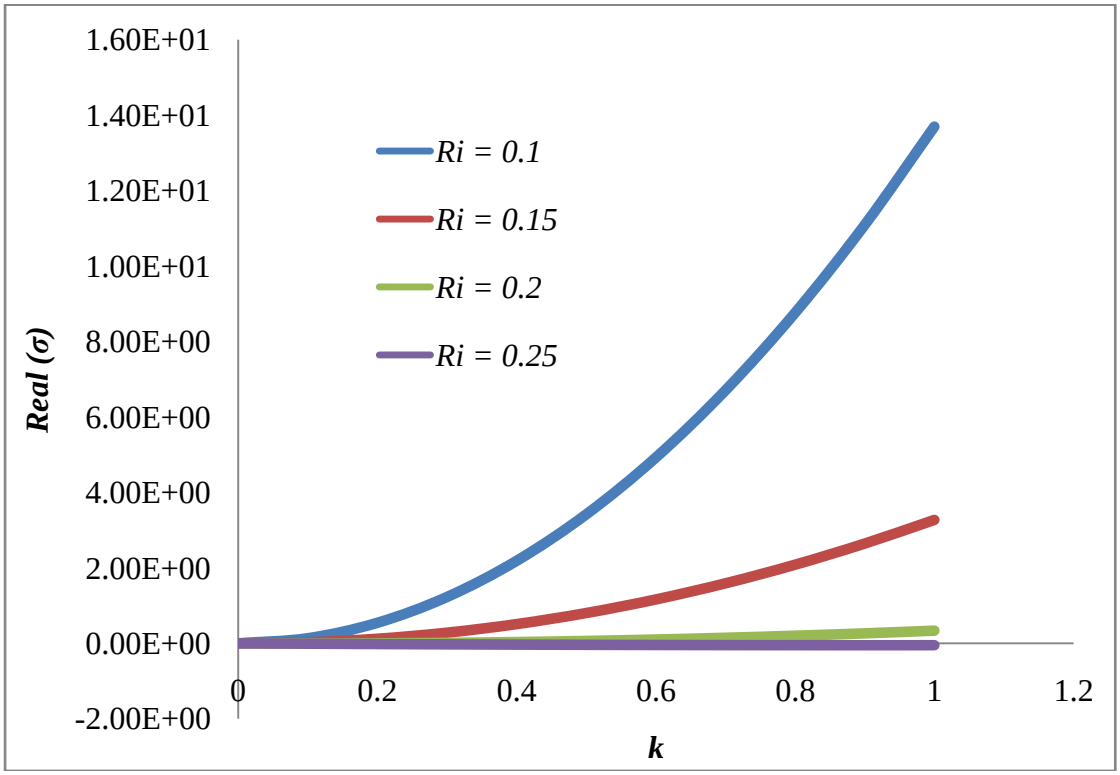

Figure 7.6 Growth rate as a function of wave number for various Ri

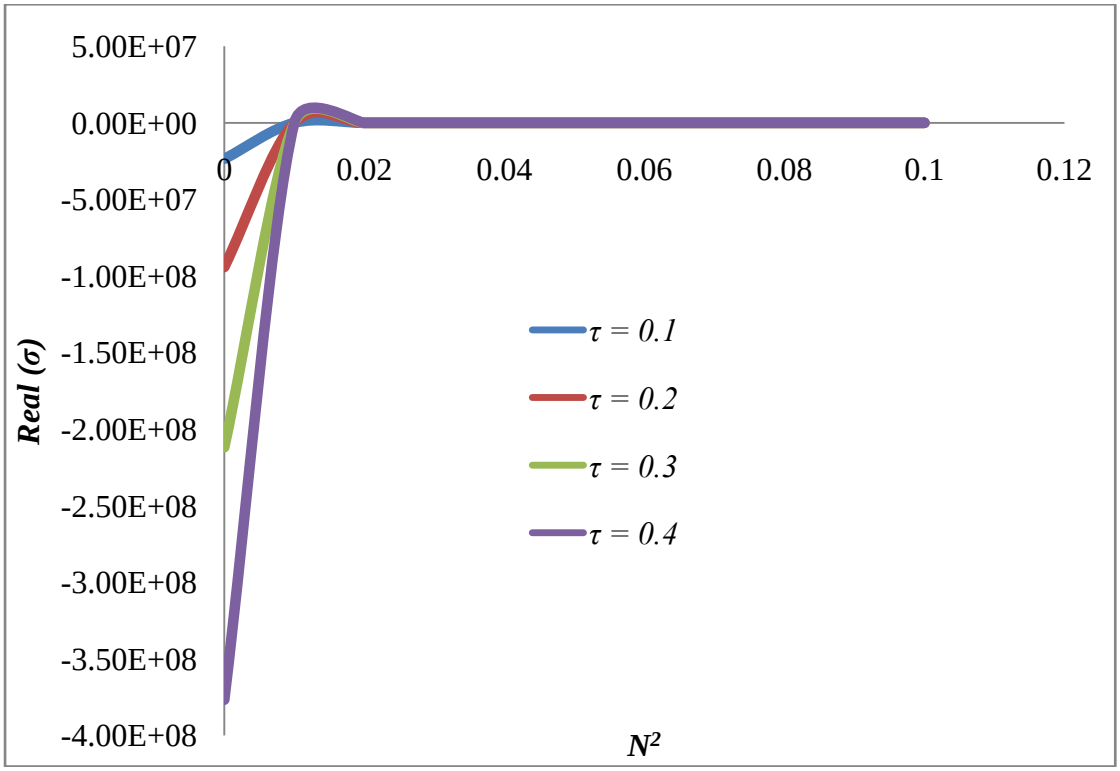

Figure 7.7 Growth rate as a function of Brunt – Vaisala frequency for various τ

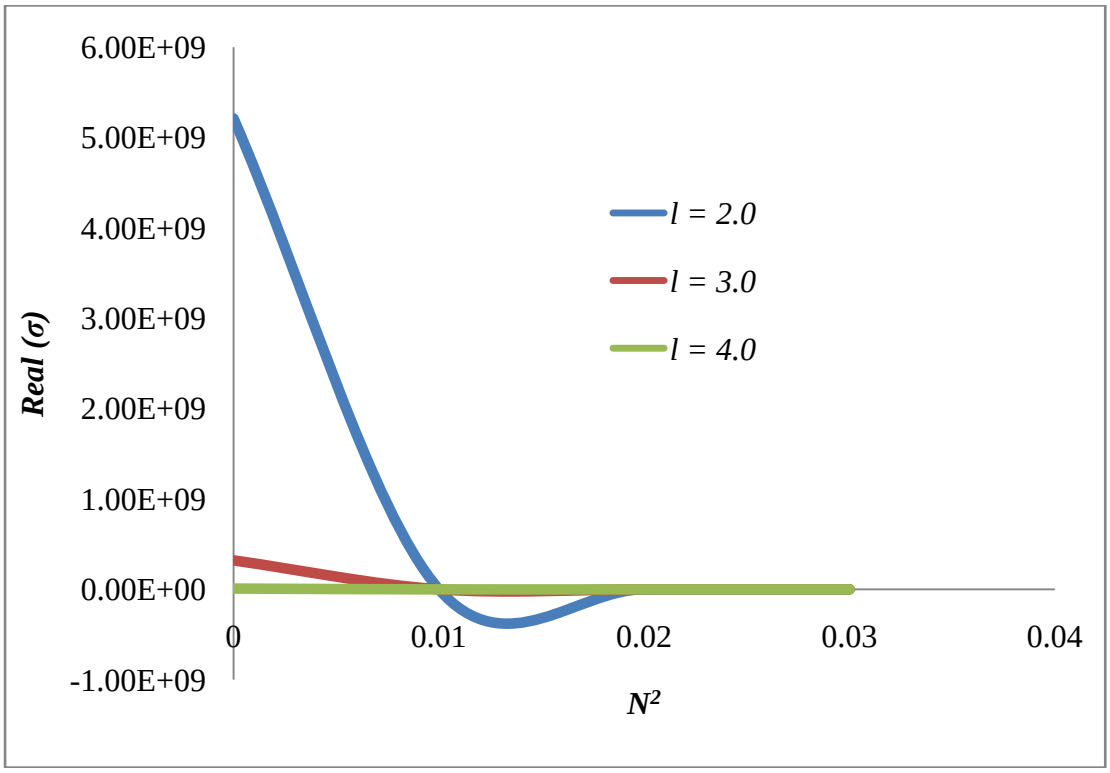

Figure 7.8 Growth rate as a function of Brunt – Vaisala frequency for various l

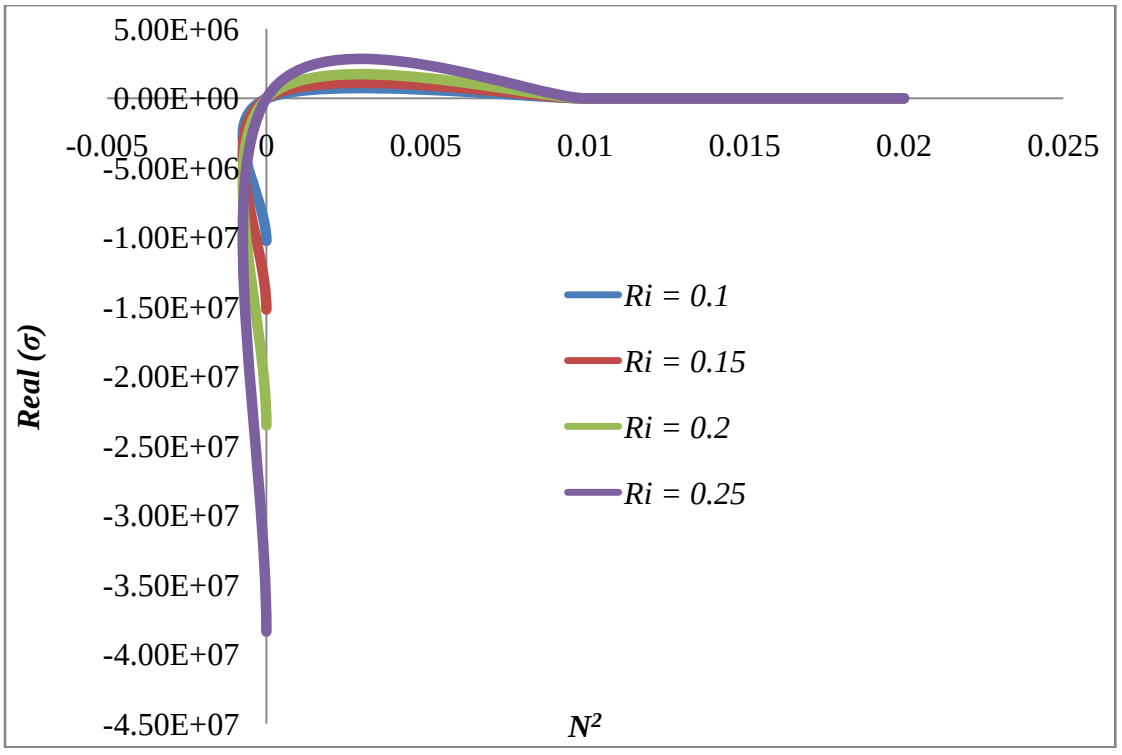

Figure 7.9 Growth rate as a function of Brunt – Vaisala frequency for various Ri

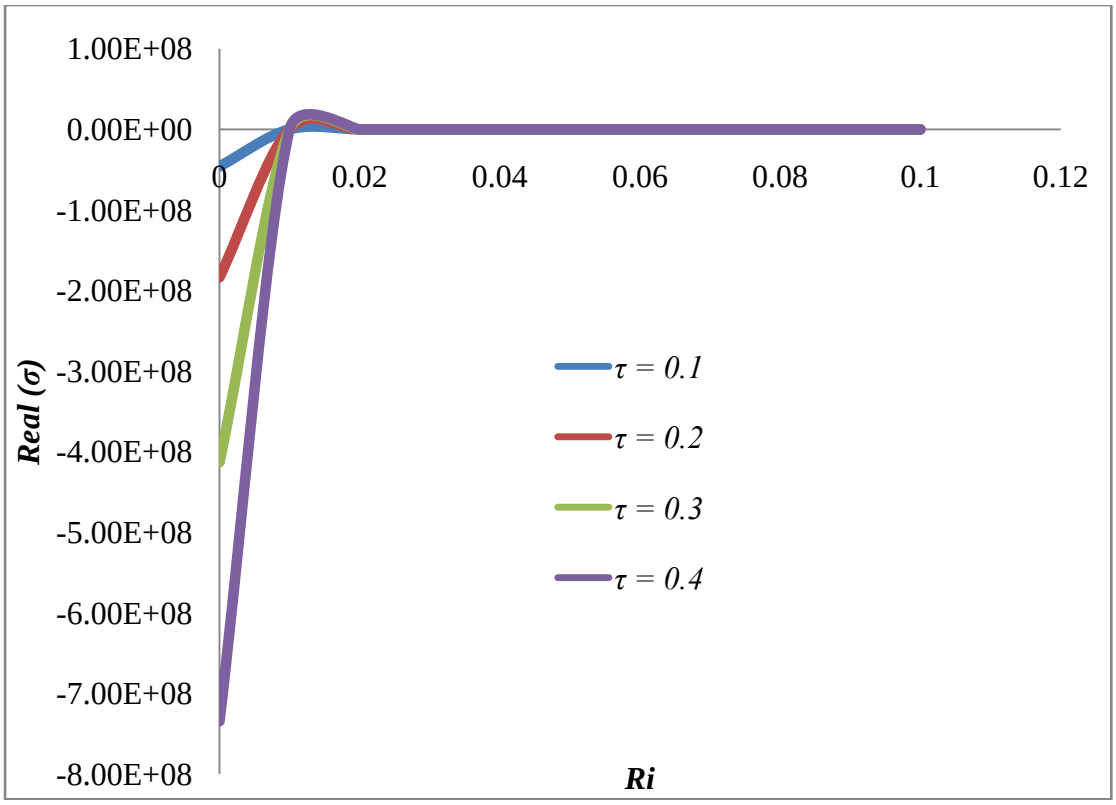

Figure 7.10 Growth rate as a function of Richardson Number for various τ

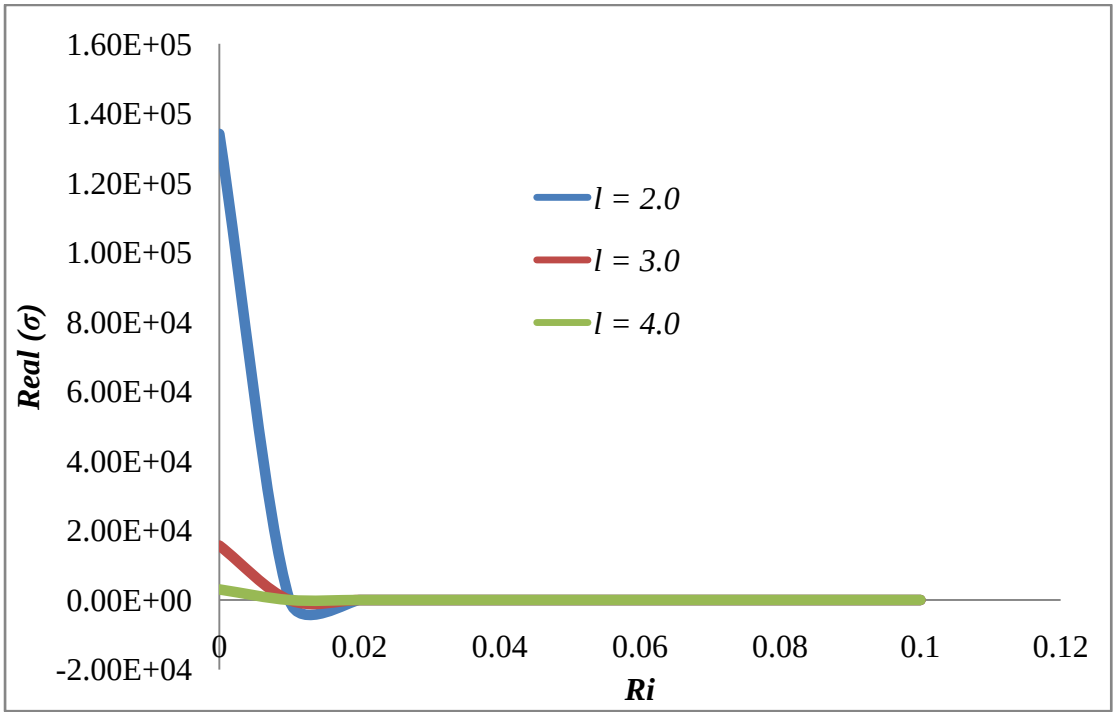

Figure 7.11 Growth rate as a function of Richardson Number for various l

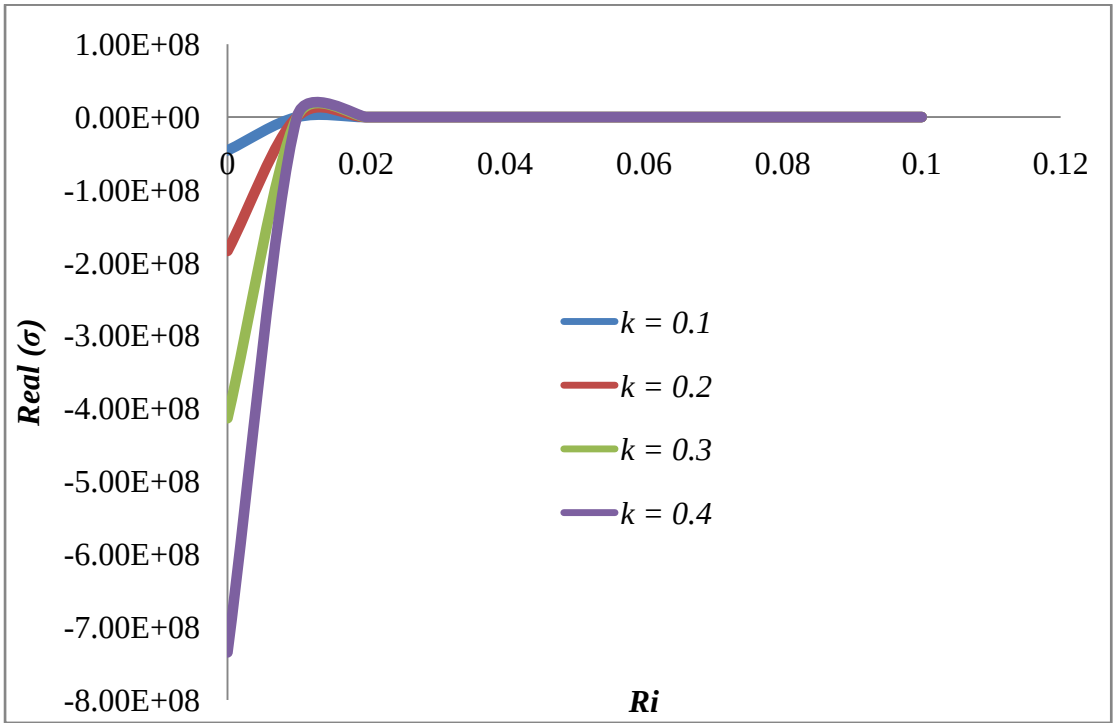

Figure 7.12 Growth rate as a function of Richardson Number for various k

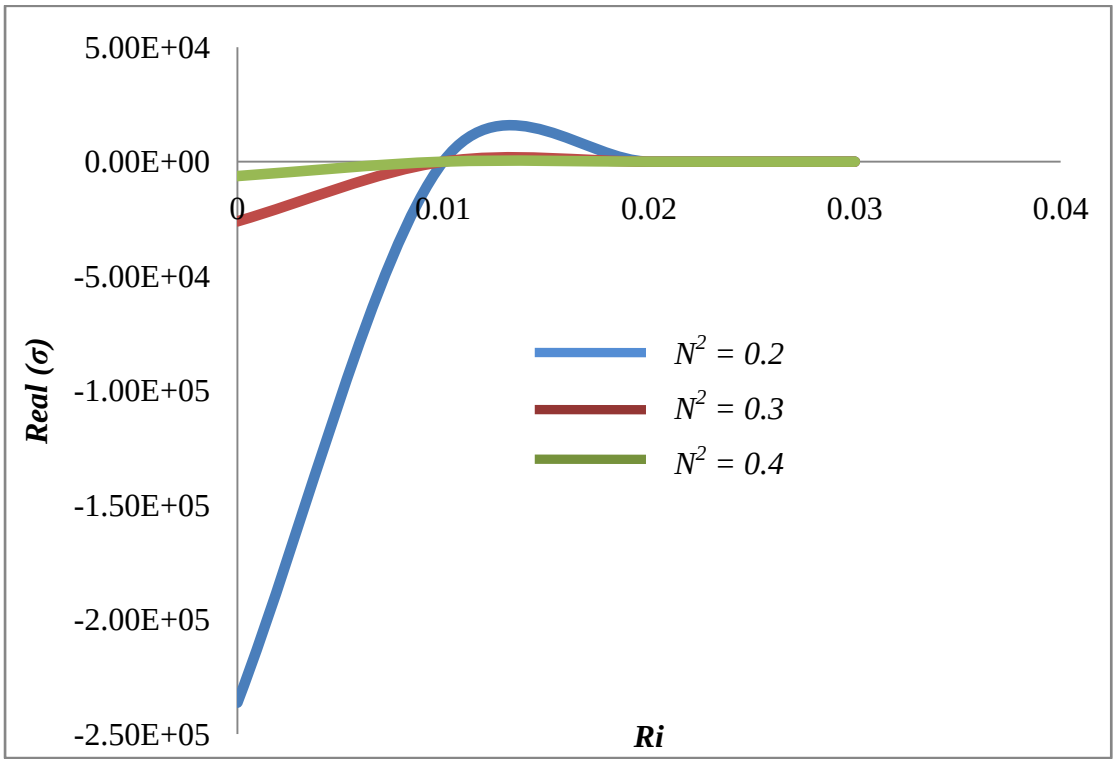

Figure 7.13 Growth rate as a function of Richardson Number for various N^2

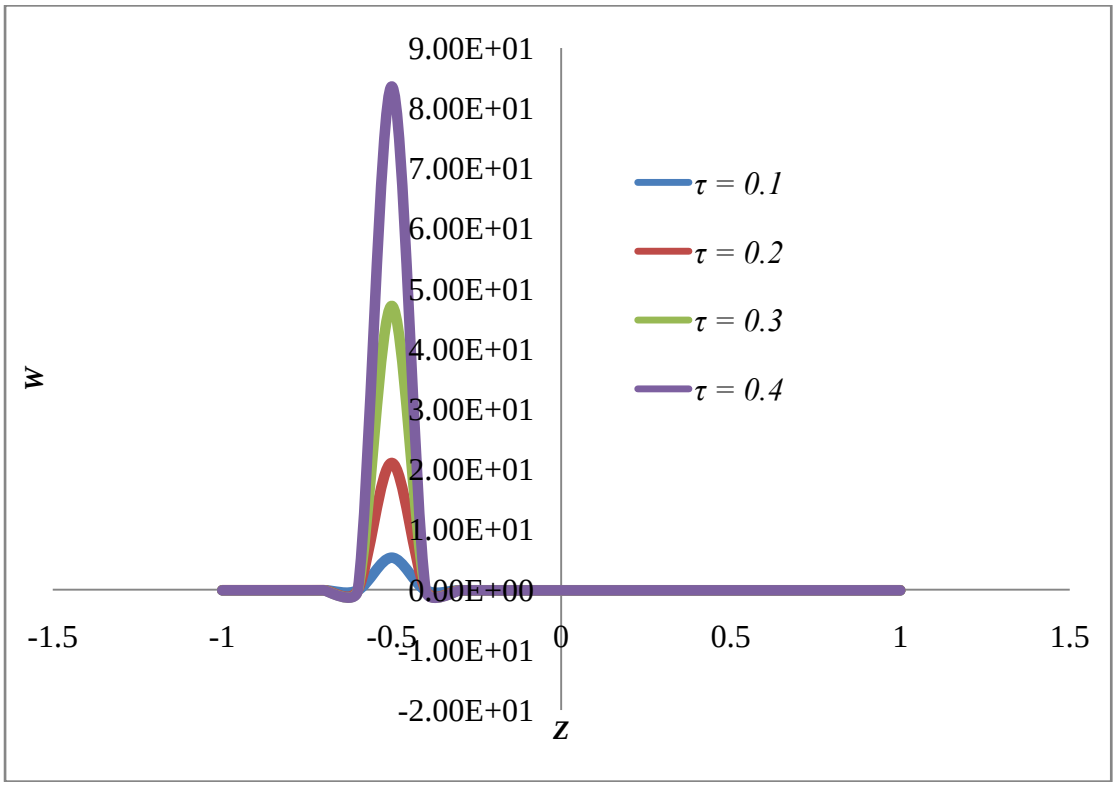

Figure 7.14 Effect of rotation number (τ) on velocity profile

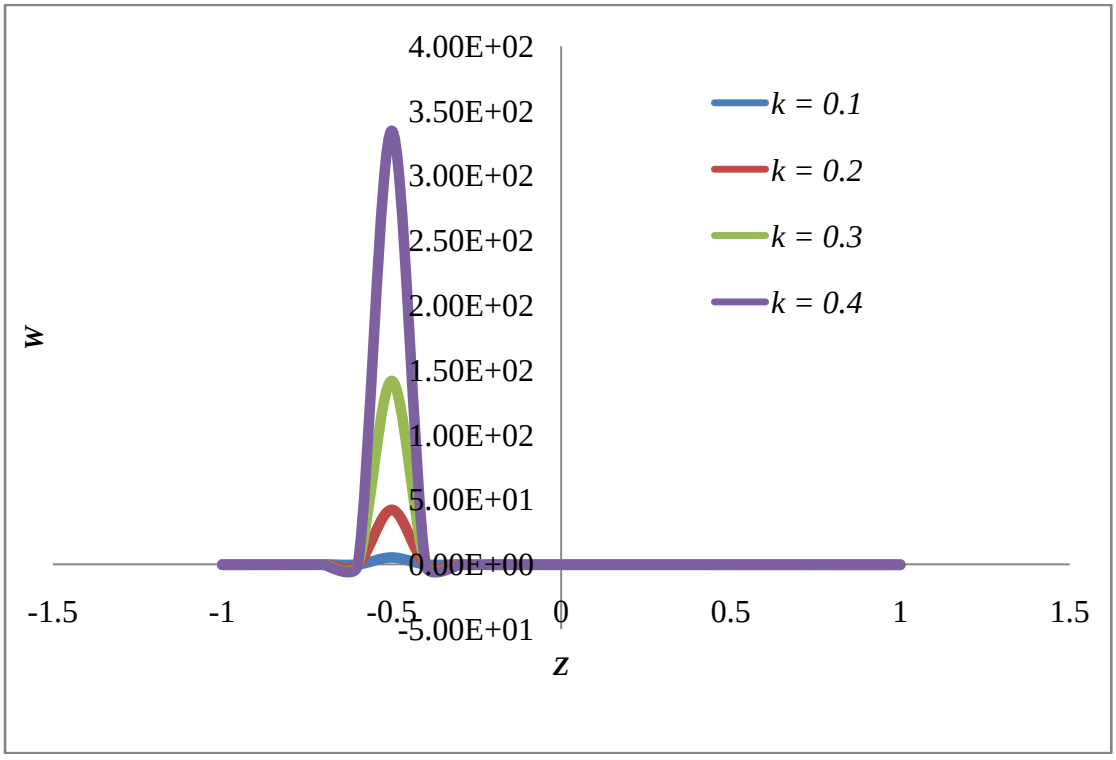

Figure 7.15 Effet of small wave number (k) on velocity profile